EFFECT OF Ni AS MINORITY ALLOYING ELEMENT ON GLASS FORMING ABILITY AND CRYSTALLIZATION BEHAVIOR OF RAPIDLY SOLIDIFIED Al-Cu-Mg-Ni RIBBONS

Vanya Dyakova[1], Yana Mourdjeva[1], Nikolay Marinkov[1, 2], Georgi Stefanov[1], Yoanna Kostova[1], Stoyko Gyurov[1]

[1]*Institute of Metal Science Equipment and Technologies with Hydro- and Aerodynamics Centre "Acad. A. Balevski" Bulgarian Academy of Sciences 67 Shipchenski Prohod Street, 1574 Sofia, Bulgaria*
[2]*Institute of General and Inorganic Chemistry Bulgarian Academy of Sciences Bl. 11 Acad. Angel Bonchev, 1113 Sofia, Bulgaria*
E-mail: v_diakova@ims.bas.bg

Received 17 January 2023
Accepted 28 February 2023

ABSTRACT

A series of rapidly solidified alloys $(Al\text{-}Cu\text{-}Mg)_{100-x}Ni_x$, x = 0, 1, 2, 3 at. % were obtained by the Chill Block Melt Spinning (CBMS). XRD and TEM analyzes showed a completely amorphous structure of the alloys. The glass transition temperature (T_g), crystallization temperature (T_x), solidus T_s and melting temperatures (liquidus) T_l were determined by DSC analyses. It was found that T_g and T_x increased with increasing the nickel content in the alloys. The reduced glass transition temperature (T_{rg}), temperature difference ΔT_x and the Hruby criterion K_H were calculated. It was found that the alloy $(Al\text{-}Cu\text{-}Mg)_{97}Ni_3$ is most thermally stable. Crystalline analogues of the amorphous alloys were obtained by annealing of melt-spun ribbons. The type and size of the separated crystal phases were determined by XRD analysis and a tendency for size diminishing with the nickel content increase was established.

Keywords: amorphous, crystallization behavior, aluminium, copper, magnesium, nickel.

INTRODUCTION

Amorphous metals have been of interest to researchers since they were synthesized in the 1960s [1] until today due to their unique properties - higher strength, lower internal friction compared to their crystalline analogues [2, 3]. Aluminium based amorphous alloys have potential applications in various fields due to their static and dynamic thermal properties [4]. Amorphous alloys are a basis for production of high-strength nanoamorphous composites that makes them promising structural materials [5]. Aluminum-based amorphous alloys are grouped into two categories: (i) Al-LTM-ETM and (ii) Al-LTM-RE, where LTM, ETM, and RE are late transition metals (LTM: Fe, Co, Ni,), early transition metals (ETM: Ti, Zr, Hf, V, Nb, Ta, Cr, Mo, W) and rare earth elements (RE: Y, La, Ce, Pr, Nd Sm, Gd, Tb, Dy , Ho, Er, Yb), that are relatively expensive. The research today is aimed at producing new chipper alloys without rare earth metals. We suppose that microalloying with small amounts of a fourth element as e.g. transition metal would enhance glass forming ability (GFA) and stabilizes the ternary amorphous alloys [6].

As a starting system for the synthesis of amorphous alloys, we have chosen the Al-Cu-Mg system because the ternary eutectic $Al_{74}Cu_{16}Mg_{10}$ vitrifies relatively easily. In previous studies, we obtained rapidly solidified ribbons (amorphous and nanocrystalline) in the Al-Cu-Mg system alloyed with different amounts of zirconium and zinc and studied their crystallization behavior [7, 8]. There are some data on the influence of Ag and Ni on the GFA of alloys of this system [9, 10]. It was established that the presence more than 5 at. % nickel improves the GFA of Al-Cu-Mg metallic glass (MG) and that Ni is the most powerful micro alloying element to increase its hardness and strength.

The aim of this work is to study the influence of nickel as a minority-alloying element on the possibility to produce amorphous alloys in the Al-Cu-Mg-Ni system, to obtain data on the crystallization behavior of the new amorphous alloys and to determine their thermal stability.

EXPERIMENTAL

Tested materials

It is known that usually the alloys have the highest GFA when their composition is close to the eutectic point [11]. For this investigation, we chose the alloy $Al_{74}Cu_{16}Mg_{10}$, which is close to point E5 of the ternary Al-Cu-Mg state diagram [12]. Small amounts of nickel were added to the ternary eutectic alloy and its influence on the glass-forming ability was investigated.

Methods of synthesis of ligatures and production of amorphous ribbons

The base $Al_{74}Cu_{16}Mg_{10}$ alloy was synthesized from pure metals Al - 99.99 %, Cu - 99.99 %, Mg - 99.8 % in a plant comprising a resistance electric furnace installed in a water-cooled pneumovacuum chamber in argon atmosphere with 99.998 % purity [7]. To each of the obtained ingots, 1, 2 and 3 at. % of high purity nickel was added, respectively. The Chill Block Melt Spinning (CBMS) method was used to obtain rapidly solidified ribbons about 3 - 4 mm wide and 26 - 40 μm thick.

In order to investigate the behavior of the base alloy and Al-Cu-Mg-Ni rapidly solidified ribbons during devitrification, samples of each type of ribbons were annealed for 2 hours at 300°C in argon atmosphere.

Characterization Methods

The chemical composition of the produced rapidly solidified ribbons was determined by Energy Dispersive X-ray Spectroscopy (EXDS) analysis using a scanning electron microscope HIROX 5500 with EXDS system BRUCKER at a magnification of 100x in 10 fields with a field area of 2.5 mm^2.

X-ray diffraction (XRD) analyses was performed to characterize the amount of amorphous and crystalline phases and to determine the phase composition of the crystalline part of the ribbons before and after devitrification with a Bruker D8 Advance powder X-ray diffractometer with CuKα radiation (Ni filter) and LynxEye recording in a solid-state position-sensitive detector. The PDF-2 (2009) database of the International Data Diffraction Center (ICDD) and the DiffracPlusEVA software package were used to perform the qualitative phase analysis.

The microstructure of Al-Cu-Mg-Ni rapidly solidified ribbons was studied by transmission electron microscope (TEM) JEOL 1011 at accelerating voltage of 100 kV. TEM foils were thinned by electrolitic jet-polishing in 40 % CH_3COON - 30 % H_3PO_4 - 20 % HNO_3 – 10 % H_2O solution.

Differential scanning calorimetry (DSC) analysis was performed on STA 449 F3 Jupiter calorimeter connected to a QMS 403 Aëolos Quadro mass spectrometer in Ar environment. The rate of the protective Ar flow in the apparatus during the analysis was 30 mL s^{-1} and the flow rate of the purge Ar through the studied samples was 20 mL s^{-1}. The heating rate was 20 K min^{-1}.

RESULTS AND DISCUSSION

The results of EXDS analyses of the chemical composition of rapidly solidified ribbons Al-Cu-Mg-Ni are presented in Table 1.

The EXDS analysis showed that the Ni content in the obtained rapidly solidified ribbons was close to 1, 2 or 3 at. % Ni, therefore, further on in our work they will be denoted respectively $(Al_{74}Cu16Mg_{10})_{100-x}Ni_x$, x

Table 1. Chemical composition of the rapidly solidified ribbons Al-Cu-Mg-Ni.

Designation of ribbons	Al, [%]		Cu, [%]		Mg, [%]		Ni, [%]	
	Mass.	At.	Mass.	At.	Mass.	At.	Mass.	At.
$Al_{74}Cu_{16}Mg_{10}$	65.04	76.60	27.63	13.82	7.33	9.59	-	-
$(Al_{74}Cu_{16}Mg_{10})_{99}Ni$	61.50	74.45	29.46	15.14	6.82	9.16	2.23	1.24
$(Al_{74}Cu_{16}Mg_{10})_{98}Ni_2$	61.28	74.54	28.84	14.90	6.38	8.61	3.50	1.96
$(Al_{74}Cu_{16}Mg_{10})_{97}Ni_3$	59.53	73.23	28.40	14.84	6.39	8.72	5.67	3.21

Table 2. Structural characteristics of amorphous and ultrafine crystalline alloys $(Al_{74}Cu_{16}Mg_{10})_{100-x}Ni_x$.

Designation of the alloy	Amorphous part	Crystal part	Components of the crystal part		
	[%]	[%]	Types of phases	Quantity of the phase [mass. %]	Phase size [nm]
$Al_{74}Cu_{16}Mg_{10}$ - am	98	2	Al Al_2CuMg	1 1	
$Al_{74}Cu_{16}Mg_{10}$ -ufcr	-	100	Al Al_2CuMg	74 26	150 60
$(Al_{74}Cu_{16}Mg_{10})_{99}Ni$ - am	100	-	-	-	-
$(Al_{74}Cu_{16}Mg_{10})_{99}Ni$ - ufcr	-	100	Al Al_2CuMg Ni_3Al+NiAl	35 46 19	177 88 69
$(Al_{74}Cu_{16}Mg_{10})_{98}Ni_2$ - am	100	-	-	-	-
$(Al_{74}Cu_{16}Mg_{10})_{98}Ni_2$ - ufcr	-	100	Al Al_2CuMg Ni_3Al+NiAl	35 44 21	139 88 44
$(Al_{74}Cu_{16}Mg_{10})_{97}Ni_3$ - am	100	0	-	-	-
$(Al_{74}Cu_{16}Mg_{10})_{97}Ni_3$ - ufcr	-	100	Al Al_2CuMg Ni_3Al+NiAl	37 45 18	136 77 27

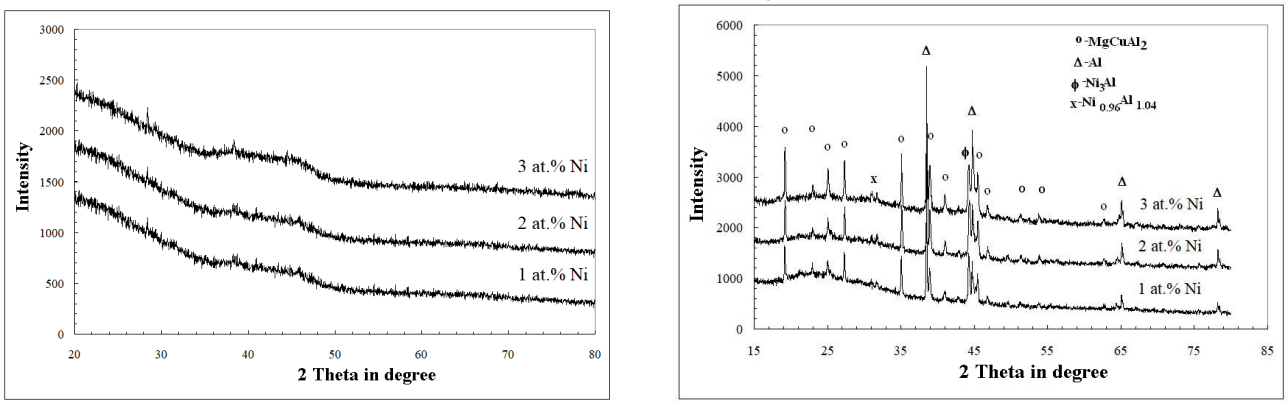

a) b)

Fig. 1. XRD diagrams of $(Al_{74}Cu_{16}Mg_{10})_{100-x}Ni_x$ ribbons before (a) and after (b) annealing. a. Amorphous alloys; b. Ultrafine crystalline alloys.

= 1, 2, 3 at. %.

The XRD patterns of $(Al_{74}Cu_{16}Mg_{10})_{100-x}Ni_x$ ribbons before and after annealing and XRD-results on their structural characteristics are presented in Fig. 1 and Table 2.

A well-defined halo is present in the diffractogram of each of the three studied $(Al_{74}Cu_{16}Mg_{10})_{100-x}Ni_x$ rapidly solidified ribbons before annealing (Fig. 1(a)), which is evidence of their amorphous structure. Further, in our work, these alloys will be denoted by the index "am".

XRD analysis of the ribbons after annealing showed complete crystallization with peaks of four types of crystalline phases: Al, Al_2CuMg, Ni_3Al and NiAl (Fig. 1(b)). The quantity and the size of the separated crystalline phases were determined both as nanosized and ultrafined in all three types of annealed alloys (Table 2). This gives us the reason to designate all annealed alloys as ultrafine crystalline (crystalline

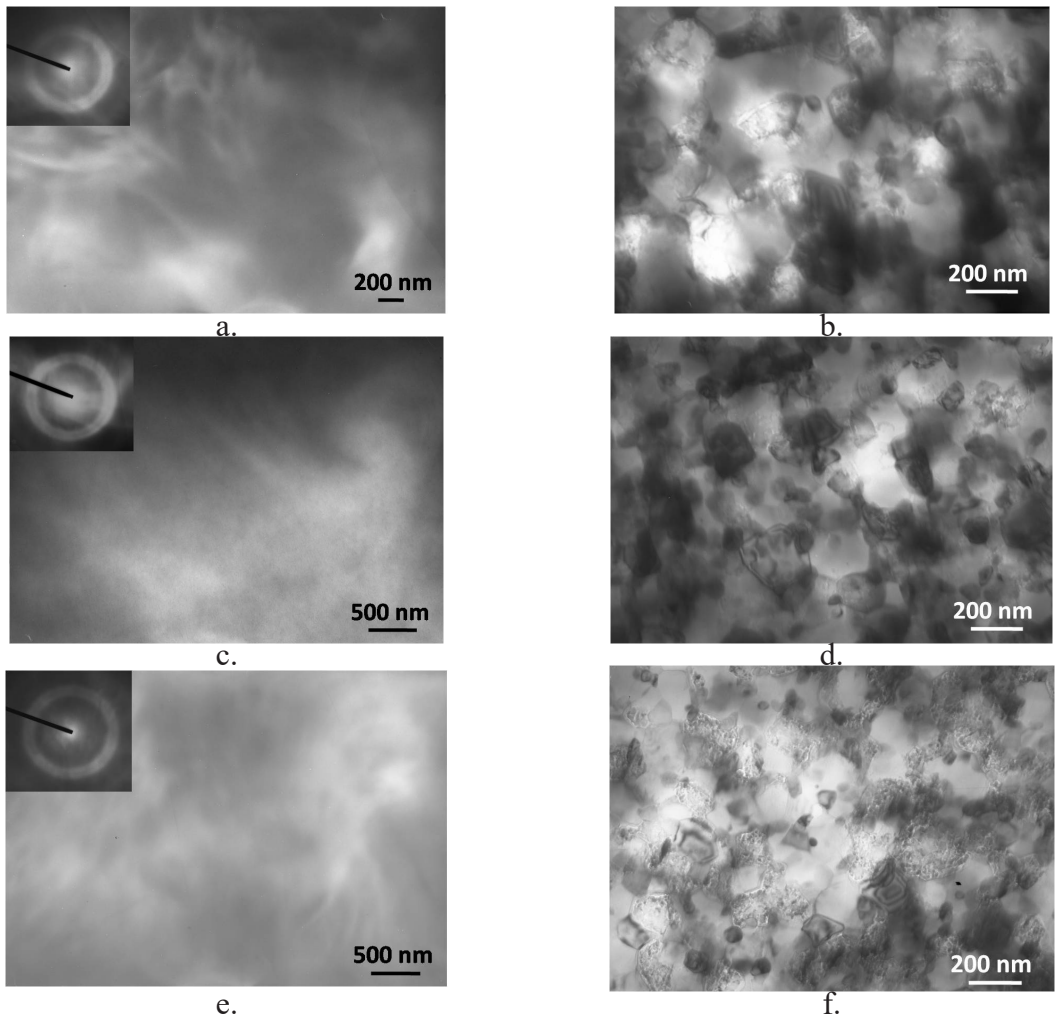

Fig. 2. Microstructure of the amorphous and ultrafine crystalline $(Al_{74}Cu_{16}Mg_{10})_{100-x}N_x$, x = 1, 2, 3 alloys, TEM.
a. Amorphous alloy $(Al_{74}Cu_{16}Mg_{10})_{99}Ni$, b. Ultrafine crystalline alloy $(Al_{74}Cu_{16}Mg_{10})_{99}Ni$, c. Amorphous alloy $(Al_{74}Cu_{16}Mg_{10})_{98}Ni_2$, d. Ultrafine crystalline alloy $Al_{74}Cu_{16}Mg_{10})_{98}Ni_2$, e. Amorphous alloy $(Al_{74}Cu_{16}Mg_{10})_{97}Ni_3$, f. Ultrafine crystalline alloy $(Al_{74}Cu_{16}Mg_{10})_{97}Ni_3$.

alloys with ultrafine grains) and to use for them the index "ufcr" [13]. In our previous studies we proved that the base rapidly solidified ribbon $Al_{74}Cu_{16}Mg_{10}$ is 98 % amorphous [7, 8]. Further, in our work we will use the obtained data to compare this base ribbon with the Ni-containing ribbons obtained in this study.

XRD results showed that the addition of only 1 at. % Ni to the amorphous base $Al_{74}Cu_{16}Mg_{10}$ alloy is sufficient to obtain a completely amorphous structure. When increasing the Ni content from 1 % to 3 % in $(Al_{74}Cu_{16}Mg_{10})_{100-x}Ni_x$ alloys, the quantitative ratio of crystalline phases content remains relatively constant: (35 - 37) % Al, (44 - 46) % Al_2CuMg, (18 - 24) % Ni_3Al+NiAl, but the grain size of all phases decreases by 25 % for Al, by 12 % for Al_2CuMg, and by 60 % for Ni_3Al+NiAl.

The results of XRD analyzes of the amorphous alloys $(Al_{74}Cu_{16}Mg_{10})_{100-x}Ni_x$ were confirmed by TEM observations and electron diffraction (Fig. 2 (a), (c), (d)). The diffractogram of the three alloys showed a well-defined diffraction halo, which proved that their structure was completely amorphous. All TEM micrographs showed uniform field with areas of varying brightness intensity, ranging from dark gray to white. We believe that the bright areas are zones with higher aluminium content, which have dissolved more intensively during the electrochemical preparation of TEM thin foils. Conversely, the darker areas on the micrographs are

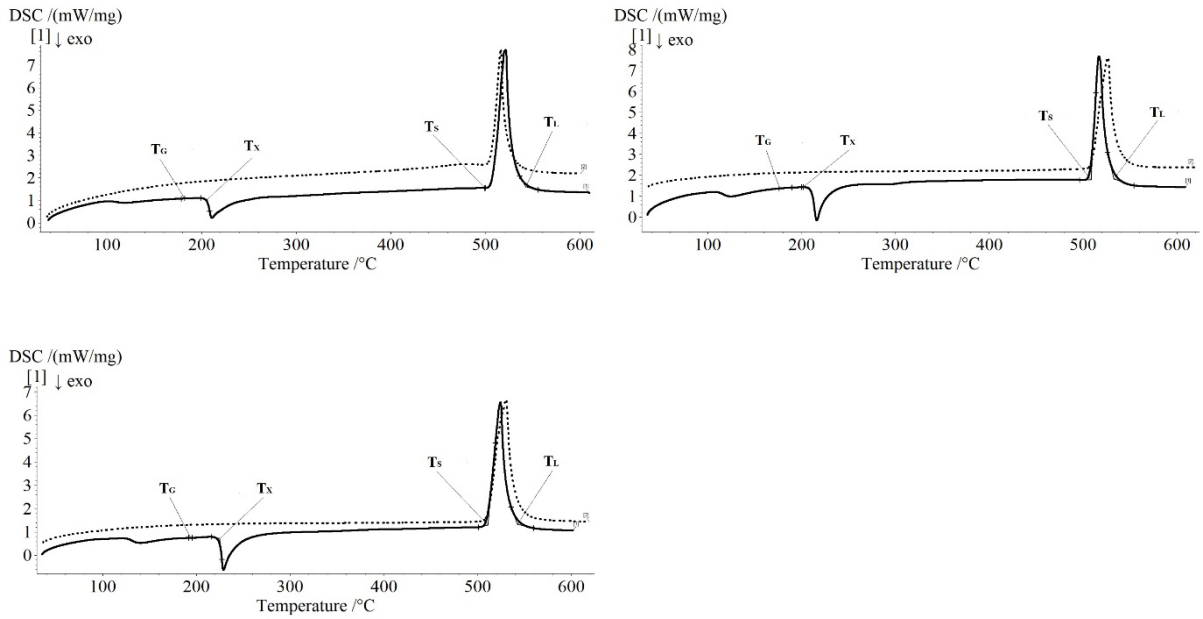

Fig. 3. DSC diagrams of the amorphous (solid line) and ultrafine crystalline (dot line) alloys. a. $(Al_{74}Cu_{16}Mg_{10})_{99}Ni$, b. $(Al_{74}Cu_{16}Mg_{10})_{98}Ni_2$, $(Al_{74}Cu_{16}Mg_{10})_{97}Ni_3$.

Table 3. Results of DSC analysis of amorphous alloys.

Designation of alloys	T_g (K)	T_x (K)	T_s (K)	T_l (K)	ΔT_x, (K)	T_{rg}	T_l-T_x	T_l-T_g	K_H
$(Al_{74}Cu_{16}Mg_{10})_{99}Ni$-am	455	479	783	805	24	0.565	326	350	$7{,}36.10^{-2}$
$(Al_{74}Cu_{16}Mg_{10})_{98}Ni_2$-am	456	484	782	803	28	0.568	319	347	$8{,}78.10^{-2}$
$(Al_{74}Cu_{16}Mg_{10})_{97}Ni_3$-am	468	499	784	811	31	0.577	312	343	$9{,}93.10^{-2}$

zones rich in copper, magnesium or nickel, which remained thicker during electropolishing. In addition, Cu and Ni are elements of higher atomic numbers, which contribute to the darker contrast also. The observation of zones of different thickness indicates to the existence of some chemical inhomogeneity of the amorphous alloys.

The microstructures of the three ultrafine crystalline alloys after devitrification by annealing are presented in Fig. 2(b), (d), (f). TEM micrographs confirm the results of XRD analysis about microstructure refinement, especially of Ni-containing phases, with the Ni content increase.

The results of the DSC analyses are presented in Fig. 3. The glass transition temperature T_g, the crystallization temperature T_x, the solidus temperature T_s and the liquidus temperature T_l, were determined and summarized in Table 3. These temperatures were found to increase with increasing nickel content in the alloys.

The crystallization of the three studied amorphous alloys $(Al_{74}Cu_{16}Mg_{10})_{100-x}Ni_x$-am, is characterized by one main exothermic peak in the temperature range (479 - 499) K, which is a proof that the alloys are in the eutectic region.

It is known that the formation of amorphous metal is more likely when the reduced glass transition temperature $Trg = Tg/Tl \geq 0.5$ [14]. In our case, the values of T_{rg} of the three studied $(Al_{74}Cu_{16}Mg_{10})_{100-x}Ni_x$ alloys are in the range (0.565 - 0.577) and slightly increase with the Ni content from 1 to 3 %. The difference ΔT_x between the crystallization temperature and the glass transition temperature $\Delta T_x = T_x - T_g$, determines the so-called supercooled liquid region of the amorphous alloy. The parameter ΔT_x is directly associated with the glass stability (GS) of the alloy and is an indication of

the resistance to devitrification by the annealing above T_g. For our amorphous ribbons the values of ΔT_x are in the range of (24 - 31) K. The thermal stability of amorphous alloys $(Al_{74}Cu_{16}Mg_{10})_{100}$-$_xNi_x$, x = 1, 2, 3 at. % was estimated according to the Hruby criterion K_H, K_H = (Tx-Tg)/(Tl-Tx) [15, 16]. According to the calculated Hruby criterion, the produced amorphous alloys are thermally stable and their resistance is comparable to the most resistant amorphous alloys [17].

Despite the relatively low value of ΔT_x the reported GFA is relatively good as Trg ≥ 0.5 and K_H has values close to 0.1. Based on the obtained results, we can conclude that all three studied alloys $(Al_{74}Cu_{16}Mg_{10})_{100-x}Ni_x$ have relatively good glass stability [18] and the most stable is the alloy with 3 at. % Ni.

The addition of even minority amounts of nickel tightens the cluster packing because of the larger atomic radius of Ni (149 pm) compared to Al (143 pm). Less free volume remains in the clusters, preventing atoms from diffusing freely and limiting both the occurrence of crystallization centres and crystal growth rates [19, 20]. The adding of larger Ni atoms in AlCuMg alloys inhibits the formation of crystalline phases in the microstructure of the amorphous rapidly solidified ribbons [19, 21]. The conclusion is that Ni is suitable for use as a minority alloying element (≤ 3 at. %) for the production of $(Al_{74}Cu_{16}Mg_{10})_{100-x}Ni_x$ amorphous alloys.

CONCLUSIONS

Rapidly solidified amorphous ribbons of 26 to 40 mm thickness based on the eutectic alloy $Al_{74}Cu_{16}Mg_{10}$ with addition of 1, 2 and 3 at. % Ni were produced. The glass transition temperature T_g, reduced glass transition temperature T_{rg}, temperature difference ΔT_x and Hruby criterion of the amorphous $(Al_{74}Cu_{16}Mg_{10})_{100-x}N_x$, x = 1, 2, 3 at. % alloys were determined. It was found that: (i) despite the completely amorphous structure, there are zones in the alloys in which Al atoms predominate, as well as zones with accumulation of Cu, Mg and Ni atoms, i.e. the amorphous alloys are not strictly chemically homogeneous; (ii) when increasing the Ni content of the alloys, the glass transition temperature T_g and the crystallization temperature T_x increase, i.e. the thermal stability of the glasses increases; (iii) the increase of Ni content refines the microstructure of the ultrafine crystalline alloys $(Al_{74}Cu_{16}Mg_{10})_{100-x}Ni_x$, x = 1, 2, 3 at. % after devitrification; (iv) Ni is suitable for use as minority alloying element (≤ 3 at. %) to produce amorphous alloys in the Al-Cu-Mg-Ni system.

Acknowledgements

This study is funded by the project "Study of the rheological and corrosion behavior of amorphous and nanocrystalline aluminum-based alloys", Contract with BNSF NoKP-06-H37/13 of 06 December 2019.

A part of experimental units used in this work was funded by the European Regional Development Fund within the OP "Science and Education for Smart Growth 2014 - 2020", project CoE "National center of mechatronics and clean technologies", No BG05M2OP001-1.001-0008-C08.

The authors are indebted to our colleges Jordan Georgiev, PhD and Ivan Penkov, PhD for their help in the preparation of the alloys and to prof. Daniela Kovacheva, PhD (Institute of Inorganic Chemistry - BAS) for the XRD analyzes of the obtained alloys

REFERENCES

1. W. Klement, R. Willens, P. Duwez, No n-crystalline Structure in Solidified Gold–Silicon Alloys, Nature, 187, 1960, 869-870.
2. H. Gleiter, Are There Ways to Synthesize Materials Beyond the Limits of Today? Metall. Mater. Trans A, 40, 2009, 1499-1509.
3. H. Jiang, T. Shang, H. Xian, B. Sun, Q. Zhang, Q. Yu, H. Bai, L. Gu, W. Wang, Structures and Functional Properties of Amorphous Alloys, Small Struct., 2, 2021, 2000057.
4. L. Drenchev, T. Spassov, G. Stefanov, A. Inoue, S. Gyurov, Static and Dynamic Thermal Properties of a Pd40Ni40Si20 Glassy Alloy, Metals, 9, 11, 2019, 1157.
5. D. Louzguine-Luzgin, Aluminum - base amorphous and nanocrysalline materials, Metal Science and heat Treatment, 53, 9-10, 2012, 472-477.
6. M. Wahid, K. Laws, M. Ferry, Effect of transition metals in the development of Al-base metallic glass, Materials Research Innovations, 17, 2013, 67-72.
7. V. Dyakova, G. Stefanov, I. Penkov, D. Kovacheva, N. Marinkov, Y. Mourdjeva, S. Gyurov, Influence of Zn on glass forming ability and crystallization behaviour of solidified Al-Cu-Mg (Zn) alloys, J.

Chem. Technol. Metall., 57, 3, 2022, 622-630.
8. V. Dyakova, G. Stefanov, D . Kovacheva, Y. Mourdjeva, N .Marinkov, I. Penkov, J. Georgiev, Influence of Zr and Zn as minority alloying elements on glass forming ability and crystallization behavior of rapidly solidified AlCuMg ribbons, 2449, AIP Conference proceedings, 2449, 2022, 060014.
9. M. Fitri, K. Laws, M. Ferry, Structural Study of Al-based Amorphous Alloy, AIP Conference Proceedings 2045, 2018, 020106.
10. M. Wahid, Processing and properties of aluminum based amorphous alloys, School of Materials Science and Engineering Faculty of Science, Doctor of Philosophy Thesis, UNSWE, Australia, 2014.
11. H. Sheng, W. Luo, F. Alamgir, J. Bai, E. Ma, Atomic packing and short-to-medium-range order in metallic glasses, Nature, 439, 2006, 419.
12. Turnary Al-Cu-Mg diagram, ID:10.1587.2.20, MSIT Worlplace, 2003.
13. R. Birringer, H. Gleiter, P. Klein, P. Marquardt, Nanocrystalline materials an approach to a novel solid structure with gas-like disorder? Physics Letters A, 102, 8, 1984, 365-369.
14. A. Inoue, Amorphous, nanoquasicrystalline and nanocrystalline alloys in Al-based systems, Progress in Materials Science, 43, 1998, 365-520.
15. A. Hruby, Evaluation of glass-forming tendency by means of DTA, Czech. J. Phys. B, 22, 1972, 1187-1193.
16. A. Kozmidis-Petrovic, J. Sestak, Forty years of the Hruby´ glass-forming coefficient via DTA when comparing other criteria in relation to the glass stability and vitrification ability 2012, Journal of Thermal Analysis and Calorimetry, 110, 2012, 997-1004.
17. K. Russew, L. Stojanova, Glassy Metals, Springer Berlin, Heidelberg, 2016.
18. A. Inoue, T. Zhang, T. Masumoto, Glass-forming ability of alloys, J. Non-Cryst. Solids, 156-158, 1993, 473-480.
19. D. Miracle, W. Sanders, O. Senkov, The influence of efficient atomic packing on the constitution of metallic glasses, Philos. Mag. A, 83, 2003, 2409-2428.
20. K.J. Laws, , D.B. Miracle, M. Ferry, A predictive structural model for bulk metallic Glasses, Nature Communications, 6, 2015, 9123.
21. L. Lingjie, W. Jiang, W. Qing, W. Yingmin, H. Guang, D. Chuang, Packing efficiency of coordination polyhedra, Philos. Mag., 90, 2010, 3961-3973.